Available online at www.sciencedirect.com

ScienceDirect

Procedia Engineering 161 (2016) 489 – 496

Procedia Engineering

www.elsevier.com/locate/procedia

World Multidisciplinary Civil Engineering-Architecture-Urban Planning Symposium 2016, WMCAUS 2016

Influence of SPH Regularity and Parameters in Dynamic Fracture Phenomena

Martin Hušek[a,]*, Jiří Kala[a], Filip Hokeš[a], Petr Král[a]

[a] *Brno University of Technology,Faculty of Civil Engineering, Veveří 331/95, Brno 602 00, Czech Republic*

Abstract

The Smoothed Particle Hydrodynamics (SPH) method can be used with advantage in the field of fracture mechanics, which is especially true when quasi-brittle materials are involved. The advantages of the SPH method are more evident when loading speed increases and dynamic material fractures start to occur. Since the SPH method is a meshfree method, the large deformation and eventual fragmentation of material during simulations can be solved without major complications. This happens because of the phase of the SPH method in which a search is made for neighbouring particles and the constraints created between them within a chosen time interval. The number of neighbouring particles depends on the size of the area where the search takes place. This area – the support domain – may therefore be considered as one of the key control elements in simulations using the SPH method. The influence of the number of particles and their initial distribution on the results is also a question. Particle clusters (areas with increased particle concentration) may be formed in cases of poor regularity. Consequently, false (numerical) cracks which bypass these clusters may appear in the simulation. The article describes an experiment concerning the dynamic loading of concrete L-specimens simulated by the SPH method. Different density distributions and initial particle distribution regularities are chosen in the simulation. The results show that it is especially necessary for the initial configuration to exhibit regular particle distribution if simulations are to be executed successfully. False cracks tend to occur more frequently with increasing particle distribution irregularities. A certain degree of compensation can be achieved via the appropriate choice of support domain size with its variations during the simulation.

© 2016 The Authors. Published by Elsevier Ltd. This is an open access article under the CC BY-NC-ND license (http://creativecommons.org/licenses/by-nc-nd/4.0/).

Peer-review under responsibility of the organizing committee of WMCAUS 2016

Keywords: Smoothed particle hydrodynamics; nonlinear constitutive model; numerical fracture; concrete;

* Corresponding author. Tel.+420 541147131.
E-mail address: husek.m@fce.vutbr.cz

1877-7058 © 2016 The Authors. Published by Elsevier Ltd. This is an open access article under the CC BY-NC-ND license (http://creativecommons.org/licenses/by-nc-nd/4.0/).

Peer-review under responsibility of the organizing committee of WMCAUS 2016
doi:10.1016/j.proeng.2016.08.671

1. Introduction

In 1977, Gingold and Monaghan [1] and Lucy [2] introduced the meshfree method, which was originally intended for the simulation of astrophysical problems. This method, which was later named Smoothed Particle Hydrodynamics (SPH), is based on assumptions regarding the flow of Newtonian fluid – most frequently described by Navier-Stokes equations. Even though the SPH method was developed mainly for the hydrodynamics field, e.g. multiphase flow [3], it has also been adapted for related fields, e.g. research into the quasi-brittle failure of materials [4-6]. The SPH method is particularly attractive in the area of high speed stress and large deformations [7, 8]. Thanks to the approach of the SPH method, in which links are built between particles at intervals occurring with a specified frequency (e.g. simulation time steps), a virtual mesh can be created even for very highly deformed areas. In this way, fragmenting matter can also be simulated without any numerical complications [9-12]. However, in cases when the distribution of SPH particles of the original geometry is not regular, the results do not correspond with those from experiments. The size of this problem is also influenced by the density of the discretization of the continuum. In order to evaluate these dependencies, the contribution focuses on dynamic loading issues concerning concrete L-specimens which are simulated using the SPH method. In the executed simulations, the regularity of the distribution of SPH particles and its influence on the type of failure are primarily examined. Results from FEM simulations and experiments are used for comparison.

Nomenclature

a_g	maximum aggregate size
d	number of dimensions
E_c	Young's modulus of concrete
f_c	cylinder compressive strength of concrete
f_t	tensile strength of concrete
G_F	fracture energy
h	smoothing length
m_j	mass of the particle j
N	number of particles
$\boldsymbol{v}$	flow velocity vector
v_c	Poisson's ratio of concrete
W	smoothing function
$\boldsymbol{x}$	position vector
ΔV_j	finite volume of the particle j
κ	smoothing function constant
ρ	mass density
ρ_c	mass density of the concrete
ρ_j	mass density of the SPH particle j
Ω	integration domain

2. Essential formulation of the SPH method and the size of the support domain

The formulation of the SPH method is often divided into two key steps. The first step is the *integral representation* of field functions, and the second is *particle approximation*. Assuming that the finite volume ΔV_j is assigned to SPH particle j, the following relationship applies:

$$m_j = \Delta V_j \rho_j ; \tag{1}$$

where m_j and ρ_j are the weight and density of particle j. The value of the monitored quantity $f(\boldsymbol{x})$, which is the product of *integral representation* and *particle approximation* operations, can thus be written as:

$$f(\boldsymbol{x}) \approx \sum_{j=1}^{N} \frac{m_j}{\rho_j} f(\boldsymbol{x}_j) W(\boldsymbol{x} - \boldsymbol{x}_j, h); \tag{2}$$

where W is the so-called smoothing function and h is the smoothing length defining the influence area of the smoothing function W – see Fig. 1.

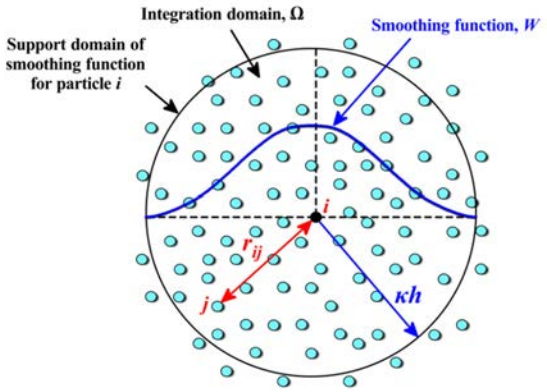

Fig. 1. Particle approximations using particles within the support domain of the smoothing function W for particle i.

The extent of the support domain is defined according to Fig. 1 as the size of the generally variable parameter h, which is called the smoothing length. Parameter h can also be multiplied by constant κ. Particles which are inside the support domain attributable to particle i are called neighbouring particles. If the resultant value of the product κh in each time step of the numerical simulation is the same, there can be the decrease in the number of neighbouring particles and thus also the decrease in the accuracy of the solution due the effect of excessive deformations (i.e. during the mutual divergence of the SPH particles). It is advisable to change the size of the support domain during the calculation in such a way that the number of neighbouring particles is constant. There are many ways to dynamically develop h so that the number of neighbouring particles remains relatively constant. In 1989, Benz [13] suggested a method of developing the smoothing length. This method uses the time derivative of the smoothing function in terms of the continuity equation

$$\frac{dh}{dt} = -\frac{1}{d}\frac{h}{\rho}\frac{d\rho}{dt} = \frac{1}{d} h \nabla \cdot \boldsymbol{v} \tag{3}$$

where $\nabla \cdot \boldsymbol{v}$ is the divergence of the flow velocity. This means that the smoothing length increases when particles separate from each other and reduces when the concentration of particles is significant. It varies in order to keep the same number of particles in the neighbourhood. Equation (3) can be discretized using SPH approximations and calculated with other differential equations in parallel [7].

3. Experiment

In 2015, Ožbolt *et al*. [14] carried out experiments during which he controlled the displacement of L-shaped concrete specimens at different speeds. The aim of the experiments and subsequent numerical simulations was to discover the dependencies between the material strength and the loading speed.

Even though displacement control speeds of 0.25 mms^{-1} – 2400 mms^{-1} were tested in the experiment, this contribution only requires attention to be paid to the highest loading speed, i.e. 2400 mms^{-1}. Fig. 2 shows a diagram of the placement of concrete specimens from the executed experiment. Fig. 3 depicts types of failure at loading speeds of 0.25 mms^{-1}, 1100 mms^{-1} and 2400 mms^{-1}. From Fig. 3 it is obvious that the type of failure also changed due to the effect of loading speed. With the change in loading speed, the resistance of the concrete specimen against deformation also changed, as did the measured maximum resistance strength – peak load. 127.73 kN was measured for a loading speed of 2400 mms^{-1}.

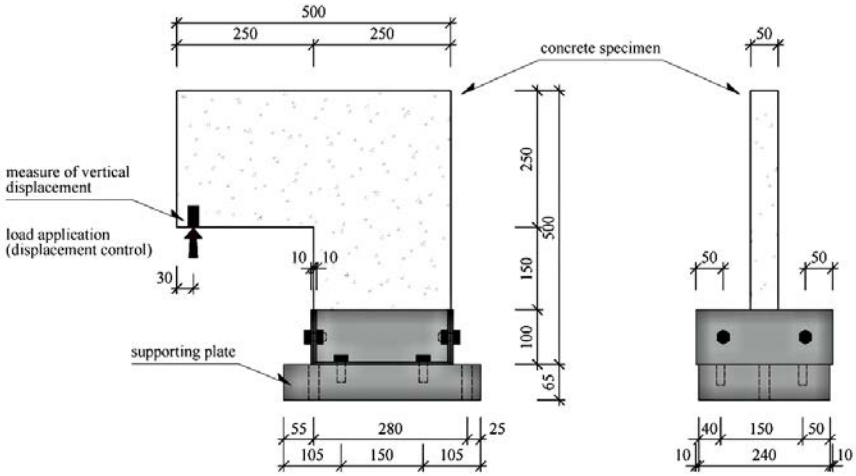

Fig. 2. Geometry and boundary conditions of the L-specimen (units in mm), [14].

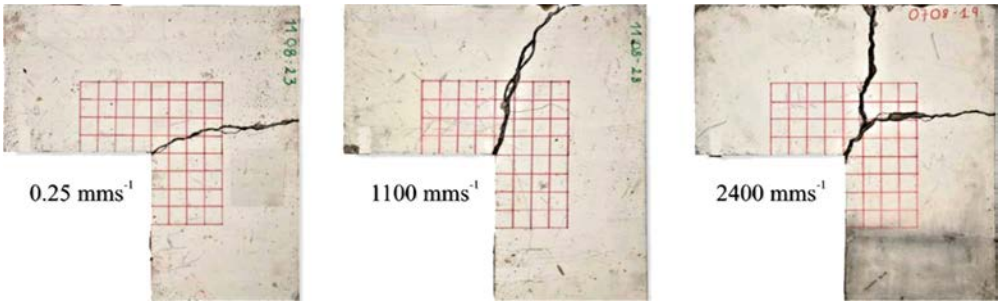

Fig. 3. L-specimen failure type for various displacement loading speeds, [14].

4. Setting up the SPH simulation

The aim of carrying out numerical simulations using the SPH method was to achieve the values measured in the experiment (for a loading speed of 2400 mms^{-1}). It was also used to obtain a corresponding failure mode to that which can be seen in Fig. 3. Simulations were carried out also using the FEM method in order to check the SPH method's results.

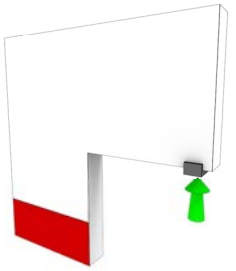

Fig. 4. Diagram of the boundary conditions of the L-specimen.

The initial geometry and placement were always the same (for all discretization variants), as can be seen in Fig. 4 where fixed FEM elements or SPH particles are shown in red. The green arrow shows the direction of loading and the grey bracket the area with loaded (displacement control) FEM elements or SPH particles. Simulations were performed in the LS-DYNA program [15].

4.1. Material model

In the numerical simulations, only the concrete specimen without steel brackets was modelled. This was done to minimize possible numerical instabilities (e. g. contacts between steel and concrete). In this way, attention could be focused exclusively on the behaviour of the SPH method. The Continuous Surface Cap Model (CSCM) was chosen as the material model of concrete to be used [16, 17]. Table 1 shows the parameters used in the simulations.

Table 1. The material parameters for the CSCM material model.

Mass density, ρ_c (kgm^{-3})	2210
Compressive strength, f_c (MPa)	46.25
Tensile strength, f_t (MPa)	3.12
Young's modulus, E_c (GPa)	32.2
Poisson's ratio, ν_c	0.18
Fracture energy, G_F (Jm^{-2})	58.56
Maximum aggregate size, a_g (mm)	8

4.2. From FEM to SPH

So that the results of the simulations of the FEM and SPH methods could be compared, FEM mesh was used as the basis for the creation of the SPH model. SPH particles were placed in the centre of gravity of the FEM elements.

5. Simulation results

In the first results section, the functionality of the FEM and SPH methods is tested for a regular mesh with different division densities. In the second results section, an area with a rougher division is inserted into the original mesh (with the finest division). In addition, this area is intentionally placed at locations through which the crack is supposed to pass, see Fig. 3, displacement loading speed 2400 mms^{-1}.

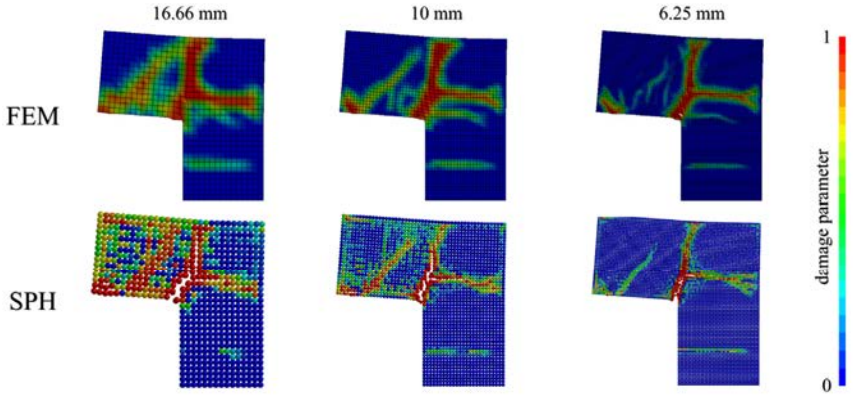

Fig. 5. Regular FEM mesh and SPH particle distribution results.

5.1. Regular mesh and density of spatial discretization

Discretization sizes of 16.66 mm, 10 mm and 6.25 mm were chosen for the FEM elements. In this way, division into 3, 5 and 8 elements were achieved along the thickness of the concrete specimen. As the SPH particles were created from FEM elements, the distances between them were also 16.66 mm, 10 mm and 6.25 mm. Figure 5 and Table 2 show the results for a regular FEM mesh and the distribution of SPH particles. The results correspond well with the experiments.

Table 2. The peak load for regular FEM mesh and SPH particle distribution.

Discretization size	FEM	SPH	experiment
16.66 mm	123.07 kN	121.06 kN	
10 mm	126.78 kN	123.07 kN	127.73 kN
6.25 mm	130.08 kN	124.18 kN	

5.2. Irregular mesh and κ parameter influence

In the second case, zones were inserted into the numerical model with element sizes of 6.25 mm where the size of the FEM mesh or the distance between the SPH particles was increased to 12.5 mm, i.e. 2x greater. With regard to this, an irregular zone of transition from size 6.25 mm to 12.5 mm was also created.

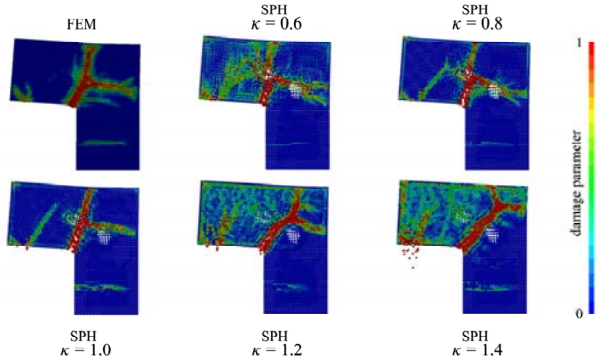

Fig. 6. Irregular FEM mesh and SPH particle distribution results.

Table 3. The peak load for irregular FEM mesh and SPH particle distribution.

κ parameter	FEM	SPH	experiment
0.6		136.00 kN	
0.8		117.39 kN	
1.0	129.13 kN	100.03 kN	127.73 kN
1.2		76.38 kN	
1.4		44.68 kN	

Figure 6 and Table 3 show the results for an irregular FEM mesh and the distribution of SPH particles. Even though the results of the FEM simulation show that the inserted irregular area does not have a significant influence either on the size of the peak load or the shape of the failure, the result is strongly dependent on the selected parameter κ in the case of the SPH method, i.e. on the size of the support domain. In the case $\kappa = 1$ it is obvious that the cracks avoid inserted areas with rougher division. Moreover, the measured strength does not correspond to the experiment. With increasing values of κ, the simulation results are increasingly different from the results of the experiment. The value $\kappa < 1$ then shows a better correspondence between the simulation and the experiment. The optimum value of κ according to Table 3 appears to be $\kappa = 0.7$.

6. Conclusions

The regularity of the distribution of SPH particles plays a significant role in simulations which use the SPH method. In the cases of poor regularity and the use of quasi-brittle materials, unreal types of crack propagation can be expected. As a rule, cracks try to avoid areas where particle clusters occur. By choosing a suitable support domain size, results which correspond to those of experiments can be achieved. The size of the support domain can be reduced via parameter κ. It is apparent that the choice of $\kappa < 1$ helps to reduce the size of the impact of poor regularity in the distribution of SPH particles.

Acknowledgements

This contribution was created with the financial aid of project GACR 14-25320S “Aspects of the use of complex nonlinear material models” provided by the Czech Science Foundation and also with support of the project FAST-J-16-3684 “Use of particle models in the concrete dynamic stress simulations” provided by the specific university research of Brno University of Technology.

References

[1] Gingold R. A., Monaghan J. J., Smoothed particle hydrodynamics: theory and application to non-spherical stars, in: *Mon. Not. R. Astron. Soc.*; 1977, vol. 181, pp. 375–389.
[2] Lucy L. B., A numerical approach to the testing of the fission hypothesis, in*: Astron. J.*; 1977, vol. 82, pp. 1013–1024.
[3] Monaghan J. J., Kocharyan A., SPH simulation of multi-phase flow, in: *Computer Physics Communication*; 1992, vol. 87, pp. 225–235.
[4] Benz W., Asphaug E., Explicit 3d continuum fracture modeling with smoothed particle hydrodynamics, in: *Proceedings of 24th Lunar and Planetary Science Conference in Lunar and Planetary Institute*; 1993, pp. 99–100.
[5] Benz W., Asphaug E., Impact simulations with fracture, in: *I methods and tests*; 1994, vol. 107, pp. 98–116.
[6] Benz W., Asphaug E., Simulations of brittle solids using Smoothed Particle Hydrodynamics, in: *Computer Physics Communications*; 1995, vol. 87, pp. 253–265.
[7] Liu G. R., Liu M. B., *Smoothed Particle Hydrodynamics: a meshfree particle method*, World Scientific Publishing Co. Pte. Ltd; 2003, 473 p., ISBN 981-238-456-1.
[8] Liu G. R., *Meshfree Methods: Moving Beyond the Finite Element Method*, New York, CRC Press; 2010, 772 p., ISBN 978-1-4200-8209-8.
[9] Kala J., Hušek M., Improved Element Erosion Function for Concrete-like Materials with the SPH Method, in: *Shock and Vibration* [online],research article, 2016, vol. 2016, article ID 4593749, 13 p., available: http://www.hindawi.com/journals/sv/aip/4593749, ISSN 1875-9203.
[10] Zukas J. A., Penetration and perforation of solids, in: *Impact dynamics*; New York, 1982, pp. 155–214.
[11] Zukas J. A., Survey of computer codes for impact simulations, in: *High velocity impact dynamics*; New York, 1990, pp. 693–714.

[12] Libersky L. D., Petscheck A. G., Smoothed particle hydrodynamics with strength of materials, in: *Proceedings of The Next Free Lagrange Conference*; New York, 1991, vol. 395, pp. 248–257.
[13] Benz W., Smoothed particle hydrodynamics: a review, in: *NATO Workshop*, Les, Arcs, France; 1989.
[14] Ožbolt J., Bede N., Sharma A., Mayer U., Dynamic fracture of concrete L-specimen: Experimental and numerical study, in: *Engineering Fracture Mechanics*; 2015, vol. 148, pp. 27–41.
[15] LSTC. *LS-DYNA Theory Manual*. Livermore, CA, USA: 2016.
[16] Murray Y. D., *User's manual for LS-DYNA concrete material model 159*. FHWA-HRT-05-062; 2007.
[17] Murray Y. D., Abu-Odeh A., Bligh R., *Evaluation of concrete material model 159*. FHWA-HRT-05-063; 2006.